

# Hysteresis in a synthetic mammalian gene network

Beat P. Kramer and Martin Fussenegger<sup>†</sup>

Institute for Chemical and Bio-Engineering, Swiss Federal Institute of Technology, Eidgenössische Technische Hochschule Hoenggerberg, HCI F115, Wolfgang-Pauli-Strasse 10, CH-8093 Zurich, Switzerland

Edited by Charles R. Cantor, Sequenom Inc., San Diego, CA, and approved May 19, 2005 (received for review January 14, 2005)

**Bistable and hysteretic switches, enabling cells to adopt multiple internal expression states in response to a single external input signal, have a pivotal impact on biological systems, ranging from cell-fate decisions to cell-cycle control. We have designed a synthetic hysteretic mammalian transcription network. A positive feedback loop, consisting of a transgene and transactivator (TA) cotranscribed by TA's cognate promoter, is repressed by constitutive expression of a macrolide-dependent transcriptional silencer, whose activity is modulated by the macrolide antibiotic erythromycin. The antibiotic concentration, at which a quasi-discontinuous switch of transgene expression occurs, depends on the history of the synthetic transcription circuitry. If the network components are imbalanced, a graded rather than a quasi-discontinuous signal integration takes place. These findings are consistent with a mathematical model. Synthetic gene networks, which are able to emulate natural gene expression behavior, may foster progress in future gene therapy and tissue engineering initiatives.**

synthetic biology | synthetic gene networks | bistability | erythromycin | feedback-loop

Hysteresis is a frequent phenomenon with implications for both everyday life as well as life sciences. Traffic jams occur when the car density exceeds a certain threshold value; return to free-flow traffic requires the car density to drop beyond a jam-triggering level (1). In biology, hysteresis plays a role in both macroscopic and microscopic events. Growth of an insect population above a certain threshold value will result in a plague of insects, the control of which requires reduction of the population size well below this threshold level (2). Furthermore, chemotactic behavior of prokaryotes resulting from direction changes of flagellar rotation follow a hysteretic switching mode (3). On a microscopic level, thermal hysteresis proteins, evolved to promote low-temperature survival of different species, lower the freezing point of H<sub>2</sub>O without significantly altering its melting characteristics (4). Hysteretic feedback control phenomena also manage glucose vs. lactose utilization preference in *Escherichia coli* (5) and ensure unidirectional cell-cycle progression in eukaryotes (6, 7).

Reductionism in the form of “-omics”-type disciplines has resulted in encyclopedic information on individual molecules and their functions. However, most biologic functions result from an interplay of several network components known as “modules.” New biological disciplines, including modular (8) and network biology (9), evolved to elucidate the general principles governing structure–function phenomena of such modules. Across disciplines, networks are known to be assembled from individual network modules or motifs. Feed-forward loops and bi-fans, known to the digital electronics community as generic circuitry modules, also operate in biological systems to control processes ranging from transcription networks to food webs (10). The system's scope of information flow across a cell's molecular networks compares in complexity and architecture with computer chips and the Internet (9).

Whenever analytic data-based network diagrams are drawn to explain complex cellular phenomena, there is always a degree of uncertainty as to whether all of the components required to elicit a certain effect have been included. To minimize such doubt, the new synthetic biology discipline makes use of another approach to understand the molecular crosstalk of cellular networks: emulation of desired signal integration by *de novo* construction and analysis of

small transgene regulation modules (11). This strategy is compatible with mathematical modeling, because all components of synthetic networks are well characterized. Furthermore, synthetic networks can be rewired by adding or removing components or circuits to gain further insight into molecular signal integration. Synthetic biology has achieved spectacular success, including construction of epigenetic toggle switches and oscillators (12–14) in *E. coli* and epigenetic transgene expression imprinting in mammalian cells (15).

Networks containing positive feedback control enable two-level expression states with hysteretic (16, 17) or bistable (18, 19) switching characteristics. Bistable expression switches quasi-discontinuously flip from OFF to ON and from ON to OFF states once a controlling stimulus reaches a specific threshold (20) (Fig. 1A). However, hysteresis requires a bigger signal to switch from OFF to ON compared with the ON-to-OFF switch. Therefore, hysteretic expression readout depends on the integration of current as well as historic input signals (Fig. 1B). The most extreme form of hysteresis is the epigenetic toggle switch, which imprints two stable expression states, even in the absence of switch-triggering signals. Endogenous and synthetic multistable expression systems have been scrutinized in *E. coli* (5, 14), which revealed that positive feedback alone was insufficient for multistability. Hysteretic networks with imbalanced expression of network components produced a graded dose-response (5), akin to systems devoid of any positive feedback loop (20) (Fig. 1C).

Capitalizing on the interconnection of tetracycline- and macrolide-responsive transgene control modalities (21, 22), we designed and characterized a synthetic mammalian gene circuitry showing hysteretic signal integration. A tetracycline-responsive positive feedback loop, communicating with a constitutive macrolide-dependent transrepressor expression unit, impinges on transcription-modulation of a desired transgene. As predicted *in silico*, the transcription readout of a well-balanced hysteretic network is either ON or OFF, depending on the presence or absence of regulating macrolide antibiotics. At macrolide concentrations around the switching dose, the network shows hysteretic expression behavior characterized by higher macrolide concentrations required for OFF-to-ON than ON-to-OFF expression changes. Because the expression output of our synthetic hysteretic network is a function of its expression history, it represents an example of artificial memory imprinted on a transgene's expression status in mammalian cells. Synthetic gene networks with hysteretic transgene expression output may be considered to be an important milestone on the path to providing prosthetic networks for gene therapy and tissue engineering in the future.

## Materials and Methods

**Plasmid Construction.** pBP228 (tetO<sub>7</sub>-ETR<sub>8</sub>-P<sub>hCMV</sub><sub>min</sub>-SEAP-IRES-tTA-pA; SEAP, human placental secreted alkaline phosphatase) was constructed by excising tTA from pSAM200 (23) by HpaI/BamHI and cloning it into the SmaI/BglII sites of pBP187

This paper was submitted directly (Track II) to the PNAS office.

Abbreviations: EM, erythromycin; SEAP, human placental secreted alkaline phosphatase.

<sup>†</sup>To whom correspondence should be addressed. E-mail: fussenegger@chem.ethz.ch.

© 2005 by The National Academy of Sciences of the USA

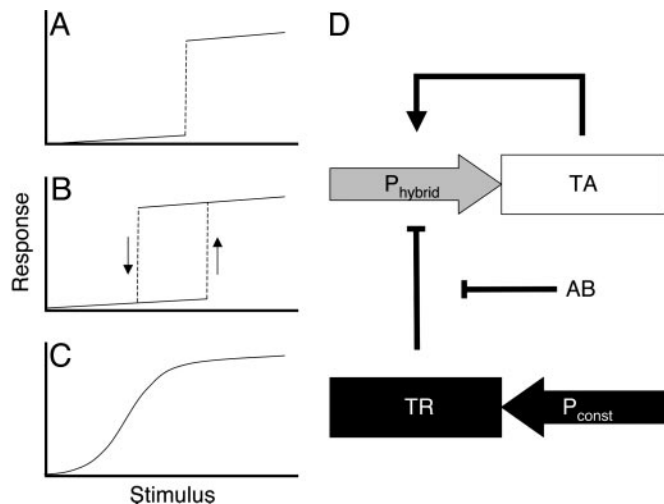


**Fig. 1.** Stimulus vs. response profiles for generic bistable (A), hysteretic (B), and graded (C) gene expression switches and schematic representation of the model hysteretic gene network (D). (A) The most basic bistable expression switch enables a quasi-discontinuous expression change between two steady states. (B) Hysteretic expression switches require a stronger stimulus for quasi-discontinuous OFF-to-ON than for ON-to-OFF expression switches. (C) A graded expression switch converts increasing stimuli to increasing responses. (D) The transactivator TA induces its own expression by means of a positive feedback loop by binding to its cognate operator contained in the hybrid promoter  $P_{\text{hybrid}}$ . The constitutively expressed transrepressor TR also binds to  $P_{\text{hybrid}}$ , thereby inhibiting TA action. Interaction of TR with an antibiotic AB abolishes TR's transrepressor capacity. Varying AB concentrations result in different active transrepressor TR concentrations and can therefore be used to fine-tune the strength of the positive feedback control unit.

[tetO<sub>7</sub>-ETR<sub>8</sub>-P<sub>hCMVmin</sub>-SEAP-IRES-pA; IRES, internal ribosome entry site of polioviral origin (24)].

**Cell Culture, Transfection, and Stable Cell Line Construction.** Chinese hamster ovary (CHO) cells CHO-WW198 (W. Weber, personal communication) and CHO-HYST were cultured in FMX-8 medium (Cell Culture Technologies, Zurich) supplemented with 5% FCS (PAA Laboratories, Linz, Austria; Catalog No. A15-022, Lot No. A01129-242) and appropriate selective antibiotics zeocin (100  $\mu\text{g/ml}$ ) (CHO-WW198, CHO-HYST) and/or blasticidin (5  $\mu\text{g/ml}$ ) (CHO-WW198). CHO-WW198 were transfected at 50% confluence by using FuGENE6 (Roche Diagnostics) according to the manufacturer's protocol by cotransfecting pBP228 and the zeocin resistance-conferring plasmid pZeoSV2 (Invitrogen) at a molar ratio of 15:1 into CHO-WW198. This pBP228:pZeoSV2 ratio increases the frequency of selected zeocin-resistant CHO-WW198 derivatives also containing cotransfected pBP228-encoded expression units. Separation of hysteretic and resistance gene expression units minimizes undesired deregulation of the antibiotic-responsive hybrid promoter by the constitutive zeocin-driving promoter without compromising the selection process (25). After a 2-week selection period (trypsinizing and reseeding after 7 days) in medium containing zeocin and blasticidin, hysteretic SEAP expression (26) of the mixed transgenic population was confirmed as outlined for individual cell clones below. The mixed cell population was subsequently diluted to five cells per ml and seeded into 96-well plates (200  $\mu\text{l}$  per well). After a 2-week incubation period in 96-well plates, supernatants of 50 clones were analyzed for SEAP expression. Positive clones were split into two wells containing zeocin and blasticidin selection medium. One of those wells was supplemented with erythromycin (EM) to assess the transgene regulation performance of individual clones. All 50 clones showed regulated SEAP expression, and CHO-HYST<sub>44</sub>, CHO-HYST<sub>42</sub>, and CHO-HYST<sub>7</sub> were chosen for further analysis.

**SEAP Assay.** SEAP production was quantified in cell culture supernatants as described in ref. 26. The SEAP detection limit is 400 nanounits/liter (27).

**Quantitative RT-PCR.** Total RNA was isolated with the NucleoSpin RNA II kit (Macherey-Nagel, Oensingen, Switzerland) from 10<sup>6</sup> CHO-HYST<sub>7/42/44</sub> cells according to the manufacturer's protocol. Two micrograms of total RNA was reverse transcribed into cDNA in a 100- $\mu\text{l}$  reaction by using TaqMan reverse transcription reagents (Applied Biosystems). Relative quantification of tTA mRNA in CHO-HYST clones was performed in a 25- $\mu\text{l}$  reaction combining the ddCT method, a tTA-specific transcript assay (Applied Biosystems; forward primer, 5'-AAGTGGGTCCGCGTACAG-3'; reverse primer, 5'-AGCAGGCCCTCGATGGTA-3'; probe, 5'-ACCCGTAATTGTTTTTCG-3'), 100 ng of cDNA, and Applied Biosystems 7500 real-time PCR equipment (Applied Biosystems) following suppliers' instructions. Standardized quantification of endogenous 18s-RNA levels ensured appropriate internal controls (Applied Biosystems, product ID Hs99999901.s1).

**Regulating Antibiotics.** EM (Fluka) was prepared as stock solutions of 1, 0.1, and 0.01 mg/ml in ethanol and used at final concentrations of 0, 125, 250, 500, 750, 1,000, 1,500, and 2,000 ng/ml.

**Modeling.** BERKELEY MADONNA software (www.berkeleymadonna.com) was used to solve model equations and generate parameter plots, and MATHEMATICA 5.0 (Wolfram Research, Champaign, IL) was applied to design simulations shown in Fig. 2.

## Results

**Qualitative Model.** The synthetic hysteretic gene network has the following setup (Fig. 1D): A transactivator (TA) activates its own transcription by binding to a chimeric promoter ( $P_{\text{hybrid}}$ ), which also can be repressed by a specific constitutively expressed [constitutive promoter ( $P_{\text{const}}$ )-driven] transrepressor (TR) whose activity is modulated by a clinically licensed antibiotic. TA as well as TR bind to their specific palindromic operator within  $P_{\text{hybrid}}$  in a cooperative manner. In the absence of antibiotics, transactivator and transrepressor bind to their operator. In such a situation, the transrepressor action dominates over transactivator function (24). The behavior of the hysteretic gene network can be described by using the following dimensionless equation:

$$d[\text{TA}]/dt = p \times [\text{TA}]^2 / (1 + [\text{TA}]^2) \times (1 - [\text{TA}]/2.5) \times 1 / (1 + [\text{TR}]^2) - \text{deg} \times [\text{TA}], \quad [1]$$

where [TA] is the concentration of the transactivator TA,  $p$  is the strength of  $P_{\text{hybrid}}$ , [TR] is the concentration of active (not inactivated by antibiotic) transrepressor molecules, and  $\text{deg}$  is the degradation rate of TA. The term  $[\text{TA}]^2 / (1 + [\text{TA}]^2)$  describes TA-mediated induction of positive feedback control. The exponent 2 reflects cooperative binding of TA dimers to their palindromic binding sites. The maximum intracellular [TA] is subject to physiologic constraints, which are considered by the term  $(1 - [\text{TA}]/2.5)$  to limit [TA] to an arbitrary unit of 2.5. The term  $1 / (1 + [\text{TR}]^2)$  reflects the repression of the hybrid promoter by TR. TA degradation depends on its degradation rate  $\text{deg}$ . Below, we define  $[\text{TA}]_0$  as the initial [TA],  $[\text{TA}]_{\downarrow}$  as the state at which TA expression is OFF, and  $[\text{TA}]_{\uparrow}$  as the state at which TA expression is ON.

To analyze the geometric structure of the model, the nullclines of Eq. 1 were determined as follows. First,  $d[\text{TA}]/dt$  was set to 0, from which follows:

$$\text{deg} \times [\text{TA}] = p \times [\text{TA}]^2 / (1 + [\text{TA}]^2) \times (1 - [\text{TA}]/2.5) \times 1 / (1 + [\text{TR}]^2). \quad [2]$$

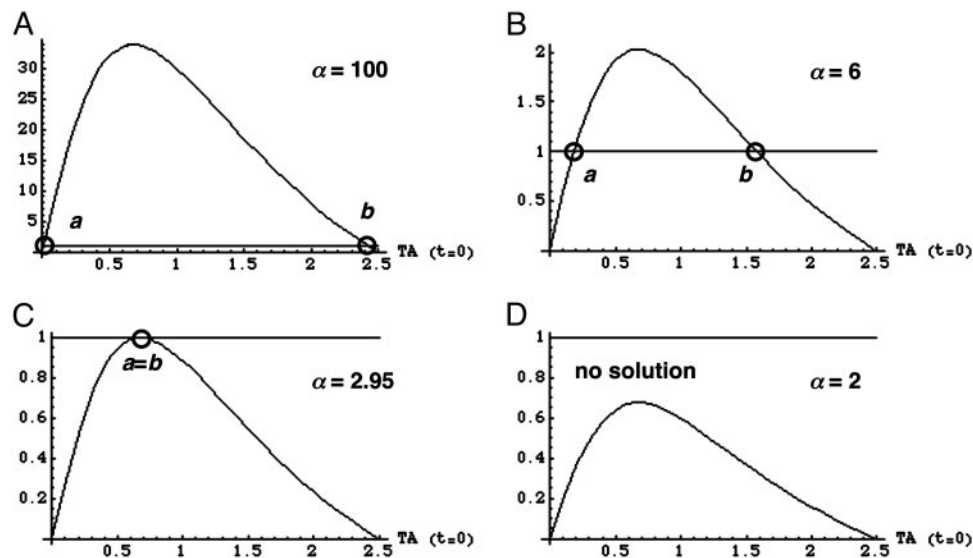


**Fig. 2.** Graphic plot of the left- and right-hand side of Eq. 4. For a given  $\alpha$  (which indirectly represents transrepressor concentration [TR]), the fate of the hysteretic system is determined by  $[TA]_0$ . For  $[TA]_0 > a$ , the final [TA] is  $b$ ; for  $[TA]_0 < a$ , the resulting [TA] is 0. For  $[TA]_0 = a$ , the resulting final TA remains at  $a$ , but small perturbations drive the system to either  $b$  or 0. (A) For very large  $\alpha$  (corresponding to low [TR]), the stable point  $b$  is big and the unstable solution  $a$  is close to zero. (B and C) As  $\alpha$  decreases (corresponding to an increase in [TR]), the two solutions  $a$  and  $b$  converge to coalesce into a single solution. (D) For sufficiently low  $\alpha$  (high [TR]), the final [TA] is zero for any  $[TA]_0$  because the line and the curve do not intersect.

The parameters  $\text{deg}$ ,  $p$ , and  $(1 + [TR]^2)$  were lumped together to create a new parameter  $\alpha = p/(\text{deg} \times (1 + [TR]^2))$ , resulting in

$$[TA] = [TA]^2/(1 + [TA]^2) \times (1 - [TA]/2.5) \times \alpha. \quad [3]$$

Eq. 3 has a stable fixed point at  $[TA] = 0$ . The intuitive explanation is that no positive feedback expression can be induced in the absence of TA. The other fixed points of Eq. 3 result from the solutions of

$$1 = [TA]/(1 + [TA]^2) \times (1 - [TA]/2.5) \times \alpha. \quad [4]$$

These fixed points can be found graphically by plotting the left- and the right-hand sides of Eq. 4 and by seeking for the intersections. Fig. 2 shows that there are zero, one, or two intersections, depending on the value of  $\alpha$ . Assume an  $\alpha$  for which there are two intersections  $a$  and  $b$ . As  $\alpha$  decreases, the two intersections  $a$  and  $b$  approach each other and eventually coalesce in a so-called saddle-node bifurcation (28) when the line intersects the curve tangentially. If  $\alpha$  decreases further, there are no intersections and therefore no additional solutions apart from  $[TA] = 0$ . To determine the stability, we take into account that  $[TA] = 0$  is stable (positive feedback expression fails to start in the absence of transactivator). Along the  $[TA]$ -axis, the type of stability alternates (28). Therefore,  $a$  must be unstable and  $b$  must be stable. These findings are logic if the architecture of the network is recalled. For  $[TA]_0 = 0$ , there is no transactivator that could initiate positive feedback expression. At point  $a$ , the TA degradation and production are equal. However, if  $[TA]_0$  decreases slightly, the resulting positive feedback expression is weaker and  $[TA]$  drops to  $[TA]_{\downarrow}$ . If  $[TA]_0$  increases slightly, TA production increases dramatically and  $[TA]$  increases to the new fixed point  $b$ . The unstable point  $a$  represents a threshold  $[TA]_0$ , below which  $[TA]$  drops to  $[TA]_{\downarrow}$  and above which  $[TA]$  jumps to the  $[TA]_{\uparrow}$  at  $b$ . In summary, the fate of the system is determined by  $[TA]_0$ .  $[TA]_{\uparrow}$  is achieved for  $[TA]_0 > a$ . Fig. 2 also reveals an important feature of the system. Hysteresis exclusively occurs if there are one unstable and two stable fixed points. This result is only the case if the curve intersects the line twice as in Fig. 2A and B. The basis for two intersections is a curve approaching 0 for very low and high  $[TA]$  with a maximum as shown

in Fig. 2. The shape of this curve is due to cooperative binding of the transactivator as described by the term  $[TA]^2/(1 + [TA]^2)$ . If positive feedback control were described by a Michaelis–Menten-like enzyme kinetics equation of the  $[TA]/(1 + [TA])$  type, the right-hand side of Eq. 4,  $(1/(1 + [TA]) \times (1 - [TA]/2.5) \times \alpha)$ , would be hyperbola-like and thus intersect the line only once. As a result, the system would have only one stable point. All  $[TA]_0 > 0$  would impinge on this stable point, and no hysteretic effect would be observed. Thus, cooperative binding of the TA is a prerequisite for hysteresis.

The qualitative behavior of the model remains stable within a two-orders-of-magnitude range of promoter strength and degradation rate values.

**Semiquantitative Model.** To determine whether the network behaves hysteretically,  $[TA]_0$  must be adjustable to different initial values. In the model, it is sufficient to change  $\alpha$  numerically. In an *in vivo* situation,  $[TA]_0$  is modulated by controlling the active [TR] using the antibiotic AB. To obtain a semiquantitative model, inactivation of TR by AB must be taken into account. Parameter  $\alpha$  was defined as  $\alpha = p/(\text{deg} \times (1 + [TR]^2))$ . If AB is bound to TR, then TR is inactive. The fraction  $\theta$  of a fixed [TR] bound to a varying [AB] can be described as

$$\theta = K \times [AB]/(1 + K \times [AB]), \quad [5]$$

where  $K = 1/[AB]_{1/2}$  is the inverse of the concentration, at which half of the transrepressors are bound to AB. Based on experimental data,  $[AB]_{1/2}$  was estimated to be 200 (ng/ml) for macrolide-responsive expression systems (22). The active TR concentration (with an arbitrary maximum of 10, which exceeds the maximum [TA] of 2.5 due to expression from a constitutive promoter) as a function of the antibiotic concentration is therefore

$$\begin{aligned} \text{TR}([AB]) &= 10 \times (1 - \theta) \\ &= 10 \times (1 - K \times [AB]/(1 + K \times [AB])). \quad [6] \end{aligned}$$

By feeding  $\text{TR}([AB])$  back into Eq. 1, a model with a quantitative antibiotic input concentration (ng/ml) is obtained. Yet, the model expression output is still in arbitrary units.

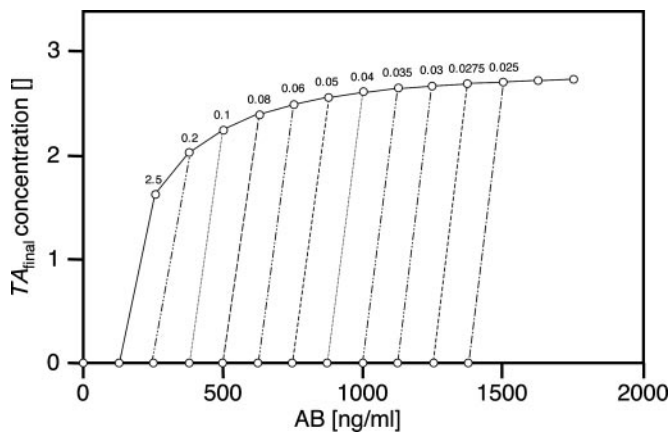


**Fig. 3.** Parameter plot showing the dependence of the final [TA] on [AB] for different [TA]<sub>0</sub>. [TA]<sub>0</sub> is crucial to determine the [AB] required to switch the system from OFF to ON. The numbers above the curve indicate for which [TA]<sub>0</sub> the final [TA] switches from OFF to ON. For example, a [TA]<sub>0</sub> of 0.08 requires an [AB] > 500 ng/ml AB for an efficient OFF-to-ON switch. Because [TA]<sub>0</sub> depends on the history of the system, the behavior is hysteretic.

$$d[TA]/dt = p \times [TA]^2 / (1 + [TA]^2) \times (1 - [TA]/2.5) / (1 + (10 \times (1 - K \times [AB]) / (1 + K \times [AB])))^2 - \text{deg} \times [TA]. \quad [7]$$

Promoter strength  $p$  was set to 1 per time unit, and TA's degradation rate was set to 0.01 (29). The mathematical model based on these parameter values predicts a final [TA] of zero for inputs of <100 ng/ml AB. If the system operates at [TA]<sup>↑</sup>, it starts switching from the ON to the OFF state at a concentration of ≈500 ng/ml AB. The antibiotic concentration at which the output of the network switches from OFF to ON depends on [TA]<sub>0</sub>. *In vivo*, [TA] will decrease to values slightly above zero due to leaky TA expression. Because the basal TA expression cannot be precisely determined, the model can only predict the emergence of hysteresis but not at which [AB] a network initially set to [TA]<sub>0</sub> will jump to [TA]<sup>↑</sup> (Fig. 3).

**In Vivo Implementation of the Synthetic Hysteretic Gene Network in CHO Cells.** The *in vivo* implementation of the synthetic hysteretic gene network was achieved as follows (Fig. 4). The tetracycline-dependent transactivator (tTA) (21) induces a hybrid promoter (tetO<sub>7</sub>-ETR<sub>8</sub>-P<sub>hCMVmin</sub>) (24) driving its own as well as SEAP expression by means of a positive feedback loop. The macrolide-dependent transrepressor (E-KRAB; ref. 22) represses tetO<sub>7</sub>-ETR<sub>8</sub>-P<sub>hCMVmin</sub>-driven transcription in an EM-responsive manner. This prototype hysteretic network was engineered on two plasmids (pBP228 and pWW198; Fig. 4) to prevent interference resulting from E-KRAB-mediated autotrans-silencing.

To characterize the synthetic hysteretic gene network, a double-transgenic cell line CHO-HYST, stably harboring pWW198 (P<sub>SV40</sub>-E-KRAB-pA) and pBP228, was constructed. For our experiments, we chose clone CHO-HYST<sub>44</sub>, whose SEAP expression was repressed by E-KRAB to undetectable levels in the absence of EM. In addition to CHO-HYST<sub>44</sub>, we selected clones CHO-HYST<sub>42</sub> and CHO-HYST<sub>7</sub>, the maximum SEAP expression levels of which were 6- and 25-fold higher compared with CHO-HYST<sub>44</sub> and could be repressed 23 ± 2-fold and 10 ± 1-fold in the presence of EM, respectively.

Because tTA and SEAP are expressed cocistronically, [tTA]<sub>0</sub><sup>↑</sup> and [tTA]<sub>0</sub><sup>↓</sup> correlates to SEAP<sub>0</sub><sup>↑</sup> and SEAP<sub>0</sub><sup>↓</sup>. CHO-HYST<sub>44</sub> was cultivated in the presence and absence of 1 μg/ml EM for 3 days to achieve SEAP<sup>↑</sup> and SEAP<sup>↓</sup>. A period of 3 days is beyond the

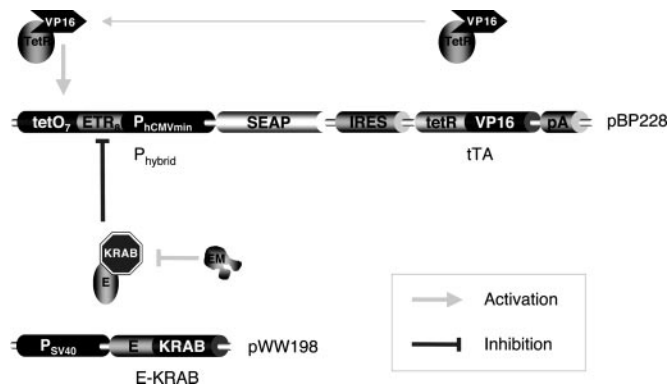


**Fig. 4.** Molecular configuration of the hysteretic synthetic mammalian gene network. The tetracycline-dependent transactivator tTA, a fusion of the *E. coli* TetR repressor and the *Herpes simplex* VP16 transactivation domain (TetR-VP16), binds to its cognate operator (tetO<sub>7</sub>) and induces the P<sub>hybrid</sub> (tetO<sub>7</sub>-ETR<sub>8</sub>-P<sub>hCMVmin</sub>)-driven dicistronic expression unit encoding SEAP and tTA, which is translated by internal ribosome entry site (IRES)-mediated translation-initiation. The transrepressor E-KRAB, a fusion of the *E. coli* macrolide resistance operon repressor E and the human transsilencing domain KRAB (E-KRAB), is constitutively expressed (P<sub>SV40</sub>-E-KRAB-pA) and binds to the ETR<sub>8</sub> operator in the absence of the regulating antibiotic EM, thereby repressing P<sub>hybrid</sub> in a dose-dependent manner.

time required to switch SEAP expression from OFF to ON or from ON to OFF (22). Cells were then trypsinized, washed twice for 20 min (to remove residual EM), and reseeded at a density of 40,000 cells per well of a 24-well plate and cultivated at different EM concentrations ([EM]). As shown in Fig. 5A, the population with an EM-free cultivation history (resulting in SEAP<sub>0</sub><sup>↓</sup>) required 1,000 ng/ml EM to completely switch SEAP expression from OFF to ON. However, CHO-HYST<sub>44</sub> populations with an EM-containing cultivation history (resulting in SEAP<sub>0</sub><sup>↑</sup>) switched SEAP expression OFF when [EM] dropped to <500 ng/ml. The response of the hysteretic gene network to different [EM] is imprinted by the population's EM cultivation history. Because SEAP expression levels for [EM] of >1,000 ng/ml are identical, a temporal effect resulting from residual SEAP in the secretory pathway preswitching cannot account for the differences in the OFF-to-ON vs. ON-to-OFF expression level of the synthetic hysteretic gene network. Such a temporal effect would have resulted in higher SEAP expression levels for cells preset in the ON state, irrespective of the [EM] after the population was split. The SEAP expression state was fully reversible and could repeatedly be switched from OFF to ON or ON to OFF (Fig. 5B).

**Fitting the Model to Experimental Data.** As mentioned above, [EM] required to switch the hysteretic gene network from OFF to ON depends on [tTA]<sub>0</sub><sup>↓</sup> after cultivation in EM-free medium. Expression data from CHO-HYST<sub>44</sub> cultivations revealed that an [EM] of 1,000 ng/ml was required to completely switch SEAP expression from the OFF to ON state. To determine which [tTA]<sub>0</sub><sup>↓</sup> would result in an OFF-to-ON expression switch at 1,000 ng/ml, a variety of parameter plots correlating [tTA]<sub>final</sub> and [EM] for different [tTA]<sub>0</sub> were generated (Fig. 3). We found that [tTA]<sub>0</sub><sup>↓</sup> up to 55-fold lower than [tTA]<sub>0</sub><sup>↑</sup> resulted in an OFF-to-ON switch at 1,000 ng/ml EM (Fig. 5A). Whenever [tTA]<sub>0</sub><sup>↓</sup> is >55 times lower compared with [tTA]<sub>0</sub><sup>↑</sup>, OFF-to-ON switches occur at higher [EM]. This simulation was confirmed by RT-PCR-based tTA-transcript quantification in CHO-HYST<sub>44</sub> ([tTA]<sub>0</sub><sup>↓</sup>/[tTA]<sub>0</sub><sup>↑</sup>, 1 ± 0.1; [tTA]<sub>0</sub><sup>↑</sup>/[tTA]<sub>0</sub><sup>↓</sup>, 54 ± 13).

**Imbalanced Building Blocks.** To determine whether cells harboring a hysteretic gene network with imbalanced expression of individual network components exhibit graded rather than hysteretic target

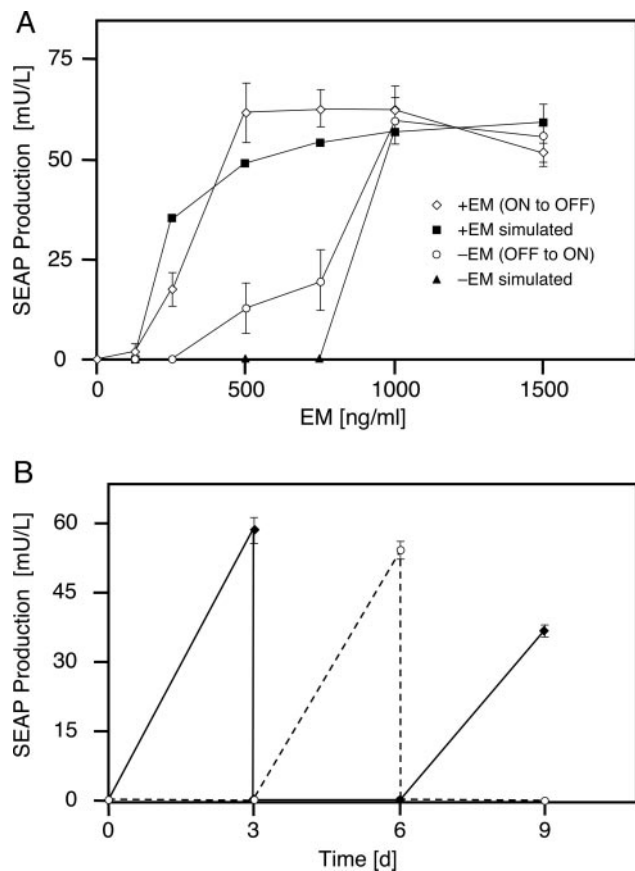


**Fig. 5.** Validation of hysteretic behavior (A) and reversibility of switching (B) of CHO-HYST<sub>44</sub>. (A) CHO-HYST<sub>44</sub> populations, double transgenic for pWW198 and pBP228, were cultivated in the presence (+) and absence (–) of EM for 3 days to set SEAP expression to an ON (+EM) or an OFF (–EM) state. The cells were then reseeded under different [EM] and assessed for SEAP production after 48 h. CHO-HYST<sub>44</sub> populations with a cultivation history in EM-free medium (SEAP production OFF) required 1,000 ng/ml EM to switch SEAP production from an OFF to an ON state, whereas CHO-HYST<sub>44</sub> populations, cultivated in the presence of EM prereseeding (SEAP production ON), switched from an ON to OFF SEAP production state at 500 ng/ml EM. The simulated curves (normalized to expression data) are shown to demonstrate the accuracy of the mathematical model. The values of [TA]<sub>0</sub> used for the simulated profiles are 2.5 (+EM) and 0.045 (–EM). (B) CHO-HYST<sub>44</sub> populations ( $5 \times 10^4$  cells) were cultivated in the presence (2  $\mu$ g/ml EM, black diamonds, solid line) and absence (dotted line) of EM. The SEAP expression status (presence of EM, ON; absence of EM, OFF) was reversed and quantified on days 3 and 6 after culture medium exchanges.

gene expression, we subjected both CHO-HYST<sub>42</sub> (intermediate-level SEAP expression; [tTA]<sub>→</sub>) and CHO-HYST<sub>7</sub> (high-level SEAP expression; [tTA]<sub>↑</sub>) to the same cultivation procedure that resulted in the data shown for CHO-HYST<sub>44</sub> (low-level SEAP expression; [tTA]<sub>↓</sub>) in Fig. 5A. The relative [tTA] in CHO-HYST<sub>7/42/44</sub> as deduced from their SEAP expression levels was confirmed by quantitative tTA transcript-specific RT-PCR (CHO-HYST<sub>44</sub>,  $1 \pm 0.2$ ; CHO-HYST<sub>42</sub>,  $2.2 \pm 0.4$ ; CHO-HYST<sub>7</sub>,  $5.4 \pm 1$ ; all tTA mRNA levels were normalized to the ones of CHO-HYST<sub>44</sub>). Although CHO-HYST<sub>42</sub> exhibited residual [EM]-imprinted hysteresis revealed by significantly different SEAP production levels within an [EM] of 125–500 ng/ml, CHO-HYST<sub>42</sub>'s dose-response characteristics had considerably shifted from a bistable to a graded response profile (Fig. 6A). In comparison with CHO-HYST<sub>44</sub> and CHO-HYST<sub>42</sub>, CHO-HYST<sub>7</sub> exhibited the highest SEAP expression ([tTA]<sub>↑</sub>). The OFF-to-ON and ON-to-OFF SEAP expression profiles of CHO-HYST<sub>7</sub> were graded between 0 and 2,000 ng/ml

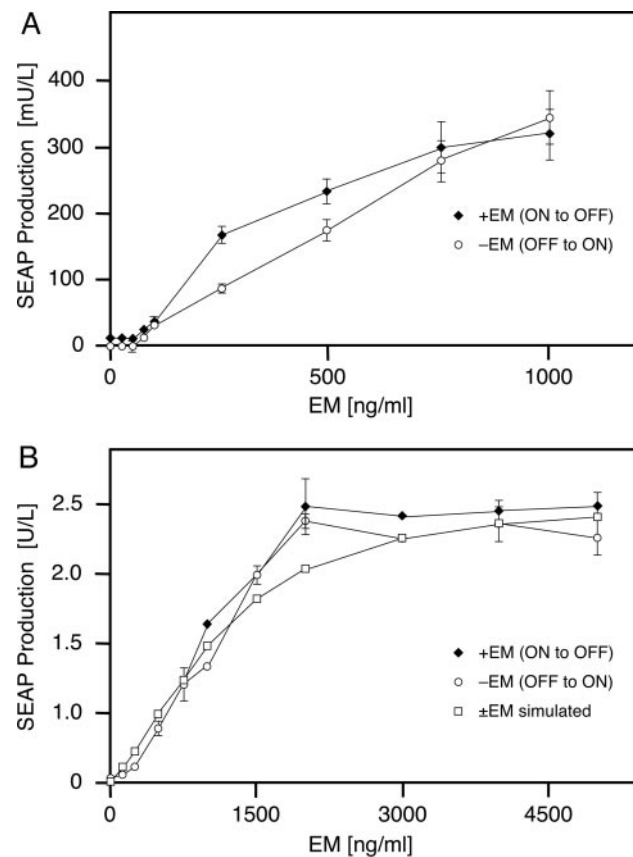


**Fig. 6.** SEAP expression profiling of CHO-HYST<sub>42</sub> (A) and CHO-HYST<sub>7</sub> (B). (A) CHO-HYST<sub>42</sub> was cultivated in the presence (+) and absence (–) of EM for 3 days to set SEAP expression to an ON (+EM) or OFF (–EM) state. The cells then were reseeded under different [EM] and assessed for SEAP production after 48 h. The SEAP expression profile of CHO-HYST<sub>42</sub> shows residual hysteresis and marks a transition state from hysteretic to graded expression response. (B) CHO-HYST<sub>7</sub> is isogenic to CHO-HYST<sub>44</sub> yet harbors imbalanced composition of hysteretic network components. CHO-HYST<sub>7</sub> was cultivated in the presence (+) and absence (–) of EM for 3 days to set SEAP expression to an ON (+EM) or OFF (–EM) state. The cells then were reseeded under different [EM] and assessed for SEAP production after 48 h. Independent of their previous incubation ( $\pm$ EM), cells reached their maximal expression gradually, after an increase in [EM] from 0 to 2,000 ng/ml. The simulated curves (normalized to expression data, identical for + and –EM) are shown to demonstrate the accuracy of the mathematical model. The values of [TA]<sub>0</sub> used for the simulated curves are 62.5 (+EM) and 6.25 (–EM).

and completely reversible without showing any signs suggestive of hysteresis. The SEAP dose-response profiles of CHO-HYST<sub>7</sub> matched those of CHO-E-SEAP, a stable EM-inducible cell line devoid of positive feedback control, at a high standard (see figure 3A in ref. 22).

Encouraged by the high degree of correlation between the model and the SEAP expression profiles of CHO-HYST<sub>44</sub>, we also tested our model for CHO-HYST<sub>7</sub>. The SEAP expression capacity of CHO-HYST<sub>7</sub> is 25 times higher compared with that of CHO-HYST<sub>44</sub>. Furthermore, SEAP expression of CHO-HYST<sub>7</sub> is only one order of magnitude below maximum expression levels, and the expression of this glycoprotein is repressed to the detection level under identical conditions in CHO-HYST<sub>44</sub>. The model Eq. 7 was adapted to account for the different expression profiles of CHO-HYST<sub>44</sub> and CHO-HYST<sub>7</sub> as follows: The maximally allowed [tTA] [characterized by the term  $(1 - [tTA]/2.5)$ ], which is the measured output in the model and is proportional to the SEAP expression *in vivo* was raised 25-fold to result in  $1 - [tTA]/62.5$ . [tTA]<sub>0</sub> values were set to the maximum level of 62.5 for pretreatment in EM-

containing medium and to 6.25 for precultivation in EM-free medium (reflecting a 10-fold reduction). A parameter plot for the final  $[tTA]$  in dependence of  $[tTA]_0$  and the current  $[EM]$  did not reveal a hysteretic effect. Independent of their cultivation history, the  $[tTA]_{0\uparrow}$  and  $[tTA]_{0\downarrow}$  populations were predicted to show identical SEAP expression profiles. Furthermore, we found that the concentration window for the ON-to-OFF switch broadened significantly, reaching a range of 0 to  $\approx 3,000$  ng/ml. Between 0 and 2,000 ng/ml, the output of the network was almost linearly dependent on the antibiotic input (Fig. 6B).

## Discussion

Transcriptional coupling of a tetracycline-dependent transactivator ( $tTA$ ), which induces its own transcription along with the transgene in a positive-feedback-loop manner, with an EM-dependent transrepressor (E-KRAB) able to repress positive feedback expression, enables hysteretic transgene control in mammalian cells. For hysteretic operation of the synthetic gene network, E-KRAB and  $tTA$  compete for  $P_{\text{hybrid}}$  interaction. At high  $[EM]$  (high levels of  $P_{\text{hybrid}}$  binding-incompetent E-KRAB),  $P_{\text{hybrid}}$ -induction is biased toward  $tTA$ , resulting in ON-to-OFF SEAP expression switches (or maintenance of high-level SEAP expression). At low  $[EM]$  (high levels of  $P_{\text{hybrid}}$  binding-competent E-KRAB), E-KRAB takes precedence over  $tTA$  for  $P_{\text{hybrid}}$  binding, which results in ON-to-OFF SEAP expression switches (or maintenance of low-level SEAP expression). Only at intermediate  $[EM]$ , when either  $tTA$  or E-KRAB may prevail for  $P_{\text{hybrid}}$  modulation and the gene network manages either high-level ( $[tTA]_{\uparrow}$ ) or low-level ( $[tTA]_{\downarrow}$ ) SEAP expression, hysteresis could occur. The resulting transgene expression state depends on  $[tTA]_0$ , which is itself a function of the cell's cultivation history. The amount of E-KRAB required to prevent induction of the  $tTA$ -dependent positive feedback loop increases with increasing  $[tTA]_0$ .

Our observation that well-balanced relative transcription factor concentrations are required to generate hysteretic target gene expression is congruent with previous findings showing conversion of hysteretic signal integration of the *E. coli* lactose utilization network into a graded response profile by providing mock lactose operators to titrate the lac repressor away from the lactose promoter (5). As exemplified by CHO-HYST<sub>44</sub>, CHO-HYST<sub>42</sub>, and CHO-HYST<sub>7</sub>, our synthetic gene network gradually changes from hysteretic to graded expression profiles the more the  $tTA$ /E-KRAB levels are biased toward  $tTA$ . Binding competition between tetracycline-dependent transactivators and

transrepressors for the same operator has been suggested to account for conversion of a graded rheostat to a bistable all-or-nothing switch (30, 31). Akin to such conversion, the bistable hysteretic network behavior (CHO-HYST<sub>44</sub>) moves toward a graded rheostat as  $tTA$  outcompetes E-KRAB for binding to the hybrid operator module (CHO-HYST<sub>7</sub>). CHO-HYST<sub>42</sub> represents a transition state characterized by a typical expression profile resulting from chimeric hysteretic-rheostat expression qualities. Besides binding competition between transcription factors, their binding kinetics were suggested to impact graded vs. all-or-nothing response profiles (32).

Transcriptional noise is known to contribute to expression heterogeneity within clonal eukaryotic populations (33). Noise intensities are typically low for fully repressed or induced expression states and become significant at intermediate expression levels (33). Because the bistable hysteretic network operates at either ON or OFF state where noise levels are considered low, noise is expected to have little impact on hysteretic network behavior. Also, all hysteretic network components are encoded on the chromosome that is known for its noise-filtering capacity (33).

The design and construction of systems that exhibit complex dynamic behavior remain the major goal of the synthetic biology community (34). An educated choice of network components as well as their assembly in precise crosstalk configurations may enable synthetic networks to increase our understanding of natural processes as well as foster therapeutic advances (14).

Positive and double-negative feedback regulation circuits, able to convert a graded into a binary response, are common control themes in nature, which evolved to manage cell fate decisions including chemotaxis, myogenesis, and cell cycle across species (19, 35, 36). Therefore, synthetic networks incorporating virus-, bacteria-, or mammalian cell-derived building blocks show a high degree of interoperability and network design principles evolved in *E. coli* also function in a mammalian cell (15). Such genericness among gene control circuitries increases hope for successful therapeutic interventions in future gene therapy and tissue engineering initiatives.

We thank Wilfried Weber (Institute for Chemical and Bio-Engineering, Eidgenössische Technische Hochschule Zurich, Zurich) for providing cell line CHO-WW198 and critical comments on the manuscript and Susanne Moelbert for help with the mathematical model. This work was supported by Swiss National Science Foundation Grant 631-065946, the Swiss State Secretariat for Education and Research within EC Framework 6, and Cistronics Cell Technology GmbH (Zurich).

- Ball, P. (2004) *Critical Mass: How One Thing Leads to Another* (William Heinemann, London).
- Ludwig, D., Jones, D. D. & Holling, C. S. (1978) *J. Anim. Ecol.* **47**, 315–332.
- Bren, A. & Eisenbach, M. (2001) *J. Mol. Biol.* **312**, 699–709.
- Barrett, J. (2001) *Int. J. Biochem. Cell Biol.* **33**, 105–117.
- Ozbudak, E. M., Thattai, M., Lim, H. N., Shraiman, B. I. & Van Oudenaarden, A. (2004) *Nature* **427**, 737–740.
- Sha, W., Moore, J., Chen, K., Lassaletta, A. D., Yi, C. S., Tyson, J. J. & Sible, J. C. (2003) *Proc. Natl. Acad. Sci. USA* **100**, 975–980.
- Tyson, J. J. & Novak, B. (2001) *J. Theor. Biol.* **210**, 249–263.
- Hartwell, L. H., Hopfield, J. J., Leibler, S. & Murray, A. W. (1999) *Nature* **402**, C47–C52.
- Barabasi, A. L. & Oltvai, Z. N. (2004) *Nat. Rev. Genet.* **5**, 101–113.
- Milo, R., Shen-Orr, S., Itzkovitz, S., Kashtan, N., Chklovskii, D. & Alon, U. (2002) *Science* **298**, 824–827.
- Hasty, J., McMillen, D. & Collins, J. J. (2002) *Nature* **420**, 224–230.
- Gardner, T. S., Cantor, C. R. & Collins, J. J. (2000) *Nature* **403**, 339–342.
- Elowitz, M. B. & Leibler, S. (2000) *Nature* **403**, 335–338.
- Atkinson, M. R., Savageau, M. A., Myers, J. T. & Ninfa, A. J. (2003) *Cell* **113**, 597–607.
- Kramer, B. P., Viretta, A. U., Daoud-El-Baba, M., Aubel, D., Weber, W. & Fussenegger, M. (2004) *Nat. Biotechnol.* **22**, 867–870.
- Angeli, D., Ferrell, J. E., Jr., & Sontag, E. D. (2004) *Proc. Natl. Acad. Sci. USA* **101**, 1822–1827.
- Xiong, W. & Ferrell, J. E., Jr. (2003) *Nature* **426**, 460–465.
- Isaacs, F. J., Hasty, J., Cantor, C. R. & Collins, J. J. (2003) *Proc. Natl. Acad. Sci. USA* **100**, 7714–7719.
- Becskei, A., Seraphin, B. & Serrano, L. (2001) *EMBO J.* **20**, 2528–2535.
- Ninfa, A. J. & Mayo, A. E. (May 11, 2004) *Sci. STKE*, 10.1126/stke.2322004pe20.
- Gossen, M. & Bujard, H. (1992) *Proc. Natl. Acad. Sci. USA* **89**, 5547–5551.
- Weber, W., Fux, C., Daoud-El-Baba, M., Keller, B., Weber, C. C., Kramer, B. P., Heinzen, C., Aubel, D., Bailey, J. E. & Fussenegger, M. (2002) *Nat. Biotechnol.* **20**, 901–907.
- Fussenegger, M., Moser, S., Mazur, X. & Bailey, J. E. (1997) *Biotechnol. Prog.* **13**, 733–740.
- Kramer, B. P., Fischer, C. & Fussenegger, M. (2004) *Biotechnol. Bioeng.* **87**, 478–484.
- Wurm, F. M. (2004) *Nat. Biotechnol.* **22**, 1393–1398.
- Schlatter, S., Rimann, M., Kelm, J. & Fussenegger, M. (2002) *Gene* **282**, 19–31.
- Berger, J., Hauber, J., Hauber, R., Geiger, R. & Cullen, B. R. (1988) *Gene* **66**, 1–10.
- Strogatz, S. H. (1994) *Nonlinear Dynamics and Chaos* (Perseus, Reading, MA).
- Pratt, J. M., Petty, J., Riba-Garcia, I., Robertson, D. H., Gaskell, S. J., Oliver, S. G. & Beynon, R. J. (2002) *Mol. Cell Proteomics* **1**, 579–591.
- Rossi, F. M., Kringstein, A. M., Spicher, A., Guicherit, O. M. & Blau, H. M. (2000) *Mol. Cell* **6**, 723–728.
- Louis, M. & Becskei, A. (July 30, 2002) *Sci. STKE*, 10.1126/stke.2002.143.pe33.
- Pirone, J. R. & Elston, T. C. (2004) *J. Theor. Biol.* **226**, 111–121.
- Blake, W. J., Kaern, M., Cantor, C. R. & Collins, J. J. (2003) *Nature* **422**, 633–637.
- Brent, R. (2004) *Nat. Biotechnol.* **22**, 1211–1214.
- Pomerening, J. R., Sontag, E. D. & Ferrell, J. E., Jr. (2003) *Nat. Cell Biol.* **5**, 346–351.
- Ferrell, J. E., Jr. (2002) *Curr. Opin. Cell Biol.* **14**, 140–148.